Journal of Inorganic and Organometallic Polymers and Materials
https://doi.org/10.1007/s10904-022-02294-0

Antibacterial and Antibiofilm Activity of Mercaptophenol Functionalized-Gold Nanorods Against a Clinical Isolate of *Methicillin-Resistant Staphylococcus aureus*

Nahla O. Eltai[1] · Nouf N. Mahmoud[2,4] · Zain Z. Zakaria[1,4] · Hana Abdelrahman[1] · Ala-Eddin Al Moustafa[1,3] · Maha Al-Asmakh[1,4]

Received: 16 December 2021 / Accepted: 8 March 2022

Abstract

Gold nanorods (AuNRs) were synthesized by the seed-mediated wet chemical method using a binary surfactant system. AuNRs were stabilized with polyethylene glycol, then functionalized with 4-mercaptophenol (4-MPH) ligand by surface ligand exchange. The surface-functionalized AuNRs (4-MPH-AuNRs) exhibited a typical UV–vis spectrum of AuNRs with a slightly shifted longitudinal peak. Furthermore, 4-MPH-AuNRs demonstrated a similar Fourier-Transformed Infrared spectrum to 4-MPH and a fading of the thiol band, which suggests a successful functionalization through thiol-gold binding. The antibacterial and antibiofilm activities of 4-MPH-AuNRs were evaluated against a clinical isolate of Methicillin-Resistant Staphylococcus aureus (MRSA). The results indicate that 4-MPH-AuNRs exhibit a bactericidal activity with a minimum inhibitory concentration (MIC) of ~ 6.25 µg/mL against a planktonic suspension of MRSA. Furthermore, 4-MPH-AuNRs resulted in a 1.8–2.9 log-cycle reduction of MRSA biofilm viable count over a concentration range of 100–6.0 µg/mL. The bacterial uptake of the surface-modified nanorods was investigated by inductively coupled plasma-optical emission spectroscopy (ICP-OES) and scanning electron microscopy (SEM) imaging; the results reveal that the nanorods were internalized into the bacterial cells after 6 h (h) of exposure. SEM imaging revealed a significant accumulation of the nanorods at the bacterial cell wall and a possible cellular internalization. Thus, 4-MPH-AuNRs can be considered a potential antibacterial agent, particularly against MRSA strain biofilms.

Keywords Gold nanorods · 4-mercaptophenol · MRSA · Antibiofilm · MIC · Bactericidal activity

1 Introduction

Antimicrobial resistance has become a challenge in treating bacterial infections, particularly those encountered in chronic wound infections; thus, there is substantial increasing demand for the development of new materials with promising antimicrobial activity against a wide range of infectious microbes [1–3].

Nanomedicine is a well-established branch of science that uses nanodevices, such as nanoparticles, acquiring unique diagnostic, biological, biotechnological, and therapeutic properties [4, 5]. Nanomaterials demonstrate several applications in electronics, catalysis, and medicine due to their exceptional physical and chemical properties [6, 7]. Recently, organic and inorganic nanomaterials have provided an alternative method to treat bacterial infectious diseases [8].

Nahla O. Eltai and Nouf N. Mahmoud have contributed equally to this work.

✉ Nouf N. Mahmoud
nouf.mahmoud@zuj.edu.jo

✉ Maha Al-Asmakh
maha.alasmakh@qu.edu.qa

[1] Biomedical Research Center, Qatar University, 2713 Doha, Qatar

[2] Faculty of Pharmacy, Al-Zaytoonah University of Jordan, Amman 11733, Jordan

[3] College of Medicine, QU Health, Qatar University, 2713 Doha, Qatar

[4] Department of Biomedical Sciences, College of Health Sciences, QU Health, Qatar University, 2713 Doha, Qatar

Published online: 06 April 2022

Among inorganic nanoparticles, gold nanoparticles (AuNPs) present with several unique physical and chemical properties, making them attractive for several biomedical applications such as sensing, imaging, diagnosis, and drug delivery and therapy [4, 9, 10]. Therefore, interest in exploiting the potential biocidal activities of AuNPs has risen recently due to their compatibility with mammalian cells, high colloidal stability, and easy conjugation to biomolecules and antibiotics [11–15]. The nanoparticles' size, shape, and surface chemistry have a crucial impact on their interaction with biological systems and cellular uptake and cytotoxicity [16–18]. Recently, Piktel et al. compared the antibacterial and antibiofilm activities of AuNPs of different shapes; they found that gold nano-peanut and AuNRs were effective against several *Escherichia coli* (*E. coli*) strains as potential antimicrobial agents for surface coatings of medical devices [13].

Surface functionalization of AuNRs is crucial to enhance their colloidal stability and reduce the concentration of toxic surfactants involved in their synthesis; furthermore, this allows the conversion of the nanoparticle to nanotherapeutics [19, 20]. We have demonstrated previously the antibacterial and antibiofilm activities of AuNRs functionalized with several chemical moieties against various gram-positive bacterial strains [21–23]. Also, we presented the utilization of AuNRs as a potential drug delivery of an anti-fungal agent [24].

Thiolated chemical molecules are commonly used to functionalize the surface of the AuNPs due to the strong binding affinity of gold towards thiol [25]. 4-mercaptophenol (4-MPH) is a small organosulfur compound that has been used in several sensing and therapeutic applications; recently, 4-MPH and thioglycolic acid-coated AuNPs were used for the detection of phytic acid and iron ions [26]. Furthermore, derivatives of 4-MPH were effective as novel anticancer agents against melanoma and breast cancer cell lines [27, 28]. In general, organosulfur compounds exhibit several biological activities, particularly antimicrobial, against a broad spectrum of bacteria, fungi, and viruses [29]; for example, 2-mercaptoethanol showed antibacterial activity towards *Propionibacterium* skin culture [30].

Among pathogens contributing to skin infections, *Staphylococcus aureus* (*S. aureus*), a gram-positive bacterium, is the most common bacterium responsible for skin and community-acquired infections. It represents a significant burden on the healthcare system [31]. *Methicillin-Resistant Staphylococcus aureus* (*MRSA)* is a resistant strain of *S. aureus*, which has a biofilm-forming ability and is considered most of the adherent *S. aureus* [32, 33] with limited options of treatment by antibiotics [34]. Bacterial biofilm is an assembly of bacterial cells attached to a surface and enclosed within extracellular polymeric substances (EPS) [35]. Due to the complex properties of biofilms, they are resistant to environmental challenges and antibiotics that complicate and limit their treatment options [35]. Nanomedicine has shown promising benefits to prevent and eradicate bacterial biofilms formation via several mechanisms [36]. AuNPs of different surface chemistries demonstrated anti-biofilm activity against various bacterial biofilms, such as *S. aureus* and *P. aeruginosa* and other types of bacterial strains [21, 37].

Surface functionalization of AuNPs with 4-MPH was investigated previously in the literature; AuNPs were functionalized with 4-MPH by surface ligand exchange due to thiol-gold binding. For example, an aqueous solution of 4-MPH was incubated directly with AuNPs solution, and the obtained 4MPH-AuNPs was characterized by Raman scattering and demonstrated pH dependence when examined by dynamic Raman scattering [38]. Similarly, aqueous solutions of 4-MPH and thioglycolic acid were added directly to AuNPs solution to form conjugated AuNPs as a colorimetric probe [39]. On the other hand, other studies followed Burst's method of synthesizing small gold nanoparticles stabilized by thiol derivatives using the two-phase liquid–liquid system [40]. However, concentrated tetrahydrofuran (THF) solution of 4-MPH was utilized for surface conjugation of AuNRs in other studies [41]; we applied a similar method in our previous study [18]. However, such methods have resulted in unstable nanoparticles in the bacterial growth media. Therefore, we introduced a new method of surface functionalization of AuNRs with 4-MPH where the nanorods were stabilized first with a low density of PEG, then conjugated with a 4-MPH by surface ligand exchange; the obtained conjugated nanorods were very stable upon mixing with the medium.

To the best of our knowledge, the antibacterial and antibiofilm activities of AuNRs functionalized with 4-MPH has not been investigated in the literature. In the current study, the antibacterial and anti-biofilm activities and bacterial uptake of the 4-MPH-AuNRs were investigated for the first time against a clinical isolate of MRSA strain.

2 Material and Methods

2.1 Synthesis and Characterization of AuNRs

2.1.1 Synthesis of AuNRs and PEG-AuNRs

AuNRs of the aspect ratio of ~ 4 were synthesized using a mixture of surfactants as described previously [42, 43]. Briefly, seed particles were synthesized by adding 0.60 mL of ice-cold sodium borohydride ($NaBH_4$ 99%, Sigma Aldrich, USA, 0.010 M) to a mixture of cetyltrimethylammonium bromide (CTAB 99%; Sigma Aldrich, USA, 0.20 M) and chloroauric acid 99.9% ($HAuCl_4$ 99%, Sigma Aldrich, USA, 0.005 M) until the formation of a light brown-colored solution. The growth solution was prepared

by adding 18 mL of silver nitrate ($AgNO_3$, Sigma Aldrich, USA, 4 mM) to a mixture of 1.234 g sodium oleate (NaOL, Sigma Aldrich, USA) and 7.0 g CTAB in 250 mL of hot water (~50 °C). After cooling down, 250 mL of $HAuCl_4$ (1 mM) was added to the growth solution and stirred for 90 min until it turned into a colorless solution. Then, a few drops of HCl 37 wt%, 0.25 mL of ascorbic acid (64 mM), and 0.8 mL of the seed solution were added to the growth solution. The obtained mixture was then incubated for 48 h at 30 °C for the slow formation of nanorods. Two-round centrifugation of the GNR suspension was performed for purification, and the pellets were dispersed in Milli-Q water. The concentration of the nanorods was estimated by inductively coupled plasma-optical emission spectroscopy (ICP-OES) at a wavelength of 242.795 nm and using a calibration curve of a gold standard (0.2–10.0 ppm, $r^2 = 0.9999$).

The synthesized nanorods were functionalized with a low density of methoxy-polyethylene glycol-thiol (m-PEG-SH, MW ~ 2000 g mol^{-1}, Sigma Aldrich, USA) to enhance their colloidal stability. A volume of 0.1 mL of a 1.0 mg/mL m-PEG-thiol solution was added to each 1.0 mL of twice-centrifuged AuNRs and left for 6 h with continuous stirring followed by centrifugation at 10,000 rpm for 10 min. The concentrated nanorods pellets were collected and dispersed in ultrapure water.

2.2 Functionalization of PEG-AuNRs with 4-Mercaptophenol (4-MPH), 4-MPH-AuNRs

The synthesized PEG-AuNRs were functionalized with 4-MPH (Sigma Aldrich, USA) by dropwise addition of 100 μL of 4-MPH (10 mM) to each 1.0 mL of twice-centrifuged nanorods; the mixture was left overnight with continuous stirring. The surface-functionalized AuNRs solution was centrifuged at 8000 rpm for 8 min to collect the nanorods pellets.

2.3 Characterization of AuNRs and 4-MPH-AuNRs

Synthesized AuNRs were characterized by UV–vis absorbance at 200–1100 nm (UV-1800 spectrophotometer, Shimadzu, Japan), surface charge, hydrodynamic size (Nicomp Nano Z3000 size/zeta potential analyzer, Entegris, USA). AuNRs samples with appropriate dilution were filled into the dynamic light scattering cuvettes for hydrodynamic radius measurement or into folded capillary cells for zeta potential measurement at 25 °C. The zeta potential of 4-MPH-AuNRs was measured upon mixing with the bacterial growth medium after 24 h of exposure. Mean values and standard deviations were calculated from at least three measurements. The shape of the nanoparticles was confirmed by transmission electron microscope (TEM) imaging (Morgani 268 TEM, FEI, The Netherlands); using Formvar coated TEM copper grids.

Surface functionalization of AuNRs with 4-MPH was also confirmed by Fourier-transformed infrared (FTIR) spectroscopy (Shimadzu, Japan). The AuNRs samples were freeze-dried and prepared as potassium bromide (KBr) disks for FTIR measurements.

2.4 Antibacterial Activity of 4-MPH-AuNRs Against *Methicillin-Resistant Staphylococcus aureus* (MRSA)

2.4.1 Bacterial Strain and Growth Condition

Clinical isolates of *Methicillin-resistant Staphylococcus aureus* (MRSA) strains were obtained from the Microbiology's bacterial culture collections at the Biomedical Research Centre (BRC), Qatar University. MRSA strains were cultured overnight on nutrient agar (Remel, ThermoFisher Scientific, Lenexa, KS, USA), incubated at 37 °C for 24 h, then adjusted to 0.5 MacFarland Standard as measured by DensiCHEK PLUS (bioMérieux, France), and used throughout the study. Longstanding preservation of cultures was done at − 80 °C in cryovial tubes (Technical Service Consultant, Lancashire, UK).

2.5 Minimal Inhibitory Concentration (MIC)

The antibacterial activity of 4-MPH-AuNRs and PEG-AuNRs suspensions was evaluated using the standard two-fold broth micro-dilution method to determine the minimal inhibitory concentration (MIC) of AuNRs against *MRSA* planktonic cultures, according to the Clinical and Laboratory Standards Institute (CLSI, 2020). Briefly, seven two-fold AuNRs suspension serial dilutions (100 µl each) were added to the wells in a 96-well flat-bottom plate ™(Microtest^{tm} 96 tissue culture plate, Franklin Lakes, NJ, USA) containing 100 µL Muller Hinton Broth (MHB, Liofilchem, Roseto degli Abruzzi, Italy) to obtain AuNRs concentration of 100, 50, 25, 12.5, 6.25, 3.12, 1.5 µg/mL. Then, 10 µL of standardized 0.5 MacFarland inoculum was added to each well within 15 min of its preparation to achieve an inoculum of 1.5×10^6 CFU/well in each well. The plate included MHB plus AuNRs as sterility controls and MHB plus *MRSA* as growth control. Finally, the inoculated 96-well plates were covered with a lid and incubated in ambient air at 37 °C for 24 h. In order to exclude the possible antibacterial activity of the coating material (4-MPH), the MIC test was performed for an aqueous dispersion of 4-MPH. MIC was recorded as the average lowest AuNRs concentration that completely inhibits *MRSA* growth as detected by the unaided eye (clear solutions). This experiment was replicated a minimum of three times.

2.6 Minimum Bactericidal Concentration (MBC)

The MBC of 4-MPH-AuNRs was determined by streaking 20 µl of a tenfold serial dilution of the MIC onto nutrient agar free from 4-MPH-AuNRs. The neutralization of the antimicrobial activity of the tested compound was achieved by dilution. The plates were then incubated at 37 °C for 16 to 18 h. Bacterial colonies, if any, were enumerated to determine viable CFU/ml. A comparable, controlled experiment was conducted as above without the application of 4-MPH-AuNRs. The number of bacterial colonies was used to calculate viable bacterial cells (CFU/ml). The percent reduction in the viable count and log reduction in viability were calculated to estimate the bactericidal activity of the 4-MPH-AuNRs [23].

2.7 Antibiofilm Activity of 4-MPH-AuNRs Against *Methicillin-resistant Staphylococcus aureus* (*MRSA*) Biofilm

2.7.1 Biofilm Culture of MRSA

Before their use, all borosilicate glass beads 3–4 mm in diameter (ISOLAB Laborgeräte GmbH, Singapore) were rinsed in a soap solution, washed in ddH2O, incubated overnight in 80% ethanol, and finally thoroughly cleaned in sterile water. Then, bacteria were cultivated on these beads as described previously [21] to form biofilm. Concisely, each bead was placed into a well in a 96- flat microtiter plate containing 200 µL of nutrient broth and 20 µL of a standardized 0.5 McFarland MRSA culture to obtain an inoculum size of 1.5×10^6 CFU/ml. Then the plates were incubated aerobically at 37 °C and 100 rpm for 72 h in a shaker incubator. After every 24 h, the consumed medium was substituted carefully by 200 µL of a new medium. After biofilm culturing, beads were washed three times using normal saline to remove loosely attached bacterial cells. Then, biofilm densities formed at 24, 48, and 72 h were determined by placing the beads in an Eppendorf tube with 200 µL of nutrient broth and vortexed for 1 min to release the attached bacteria. After that, 100 µL of the suspension was serially diluted over tenfold serial dilutions, and 20 µL was streaked on nutrient agar media. The number of colonies was reported quantitatively to determine biofilm density as CFU/bead.

2.8 Antibiofilm Activity of AuNRs Suspension Against MRSA

The antibiofilm activity of AuNRs suspension on 72-h biofilm cultures was determined by challenging the washed biofilm beads with exposure to AuNRs (100, 40, 20, and 6 μg/mL) suspension for 24 h incubation at 37 °C. After treatment, beads were washed with normal saline, and viable biofilm density was determined, as previously mentioned in Sect. 2.3.1 [21]. The antibiofilm activity was estimated as a percentage reduction of viability compared to the initial number of untreated biofilm [21].

2.9 Imaging of *MRSA* Biofilm by Scanning Electron Microscopy (SEM)

The biofilm on the glass bead was dip-washed in ddH_2O and fixed in the previously mentioned fixative for 48 h. Consequently, all samples were air-dried, mounted on a stub with adhesive carbon tape, then sputter-coated with a 12-nm layer of gold and examined by SEM (ZEISS 1530 Gemini, Carl Zeiss Microscopy GmbH, Germany) operating at 5 kV.

2.10 Quantification of Bacterial Uptake of 4-MPH-AuNRs by Inductively-Coupled Plasma- Optical Emission Spectrometry (ICP-OES)

Samples were prepared in a liquid form through digestion to produce an aqueous solution in Nitric acid. Briefly, 4.0 McFarland *MRSA* suspended in 250 µL Müller Hinton Broth was treated with 4-MPH-AuNRs (100 μg/mL) for 6 h at 37 °C and then centrifuged for 5 min at 8000 rpm. After that, the formed pellet (weight 0.19–0.20 g) was washed with 1% HNO_3, followed by five times deionized water. Consequently, the washed pellets were lyophilized by a vacuum freeze-drier (VirTis SP scientific, USA) for 30 h condensation at − 70 °C. Afterward, the samples were mixed with a concentrated nitric acid and placed on a hot block (environmental express, Charleston, South Carolina) at 105 °C for 2 h, then diluted up to 10 mL by adding distilled deionized water. The reagent blanks were treated precisely as were the samples. Then the cellular uptake of AuNRs was determined using ICP-OES (Optima, 7300 DV Perkin Elmer, South Carolina, USA).

2.11 Imaging of Bacterial Uptake of 4-MPH-AuNRs by SEM

MRSA suspension of 1.0 MacFarland (250 µL) was treated with 50 µL of 100 μg/mL of 4-MPH-AuNRs for 6 h at 37 °C. After that, the treated bacterial cells were washed with deionized water; then, the pellet was fixed with 2% glutaraldehyde. Subsequently, the sample was examined using TEM (TECNAI G2 TEM, TF20, FEI, USA).

3 Results and Discussion

3.1 Synthesis and Characterization of AuNRs

AuNPs conjugated with 4-MPH were investigated in the literature for several biomedical applications such as sensing; however, these nanoparticles' antimicrobial and antibiofilm activities, particularly non-spherical nanoparticles, have not been highlighted in the literature.

In this study, AuNRs were synthesized using a mixture of surfactants (oleic acid and cetyltrimethylammonium bromide: CTAB), to finetune the size uniformity and adjustability [43]. The synthesized nanorods were then functionalized with a low density of PEG to enhance their colloidal stability towards the next step of surface functionalization with 4-MPH and enhance the colloidal stability of the 4-MPH-AuNRs upon mixing with the bacterial growth medium (Fig. 1A).

The optical spectrum of PEG-AuNRs demonstrated two distinct peaks at 519 and 833 nm for the longitudinal and transverse peaks, respectively (Fig. 1B). The obtained surface-functionalized AuNRs (4-MPH-AuNRs) exhibited a slightly shifted and broadened longitudinal plasmon due to the change in the dielectric constant of the surrounding medium and a possible slight aggregation (Fig. 1B). The plasmon band intensity and wavelength of AuNPs depends on many factors modulating the electron charge density on the particle surface such as the particle size, shape, composition and the dielectric constant of the surrounding medium [44]. Furthermore, slight broadening of the longitudinal peak of 4-MPH-AuNRs might be related to the possible binding of the nanorods to 4-MPH through the O-AuNRs bond. A previous study showed such binding induced aggregation of the AuNPs at pH ~ 10 [38]. However, no significant difference in the hydrodynamic sizes of the nanorods before and after functionalization was observed.

TEM imaging clearly showed the nanoparticles' rod shape with an average length and width of ~ 72 nm and ~ 17 nm, respectively (Fig. 1C). The average hydrodynamic size of the nanorods measured by dynamic light scattering before

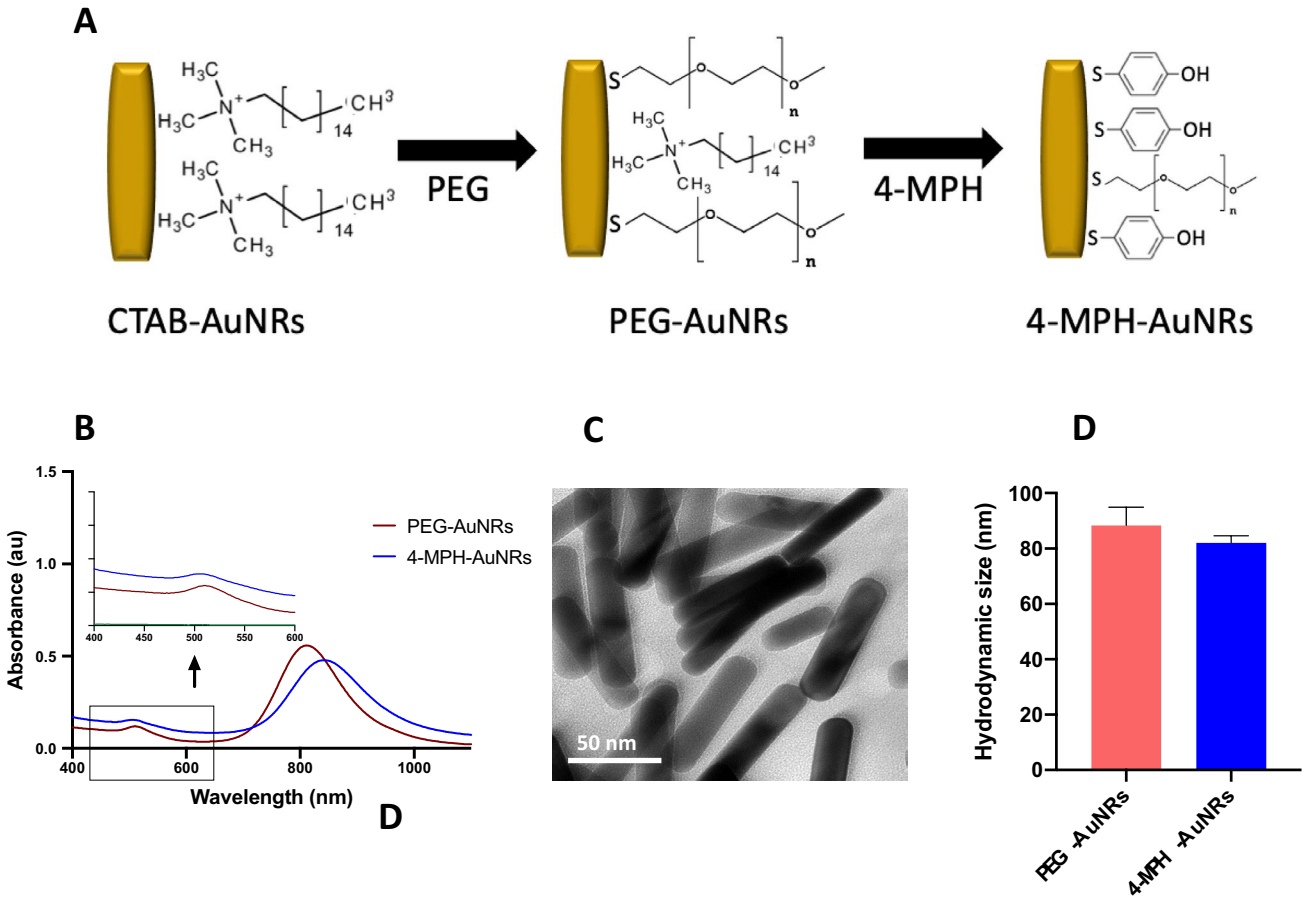

Fig. 1 **A** A scheme represents the functionalization process of AuNRs with 4-MPH. **B** UV–vis spectra of AuNRs, 4-MPH-AuNRs, and 4-MPH. **C** TEM image of 4-MPH-AuNRs. **D** Hydrodynamic size of AuNRs before and after functionalization with 4-MPH

and after functionalization was ~ 88 nm and 84 nm, respectively (Fig. 1D). The average surface charge of the nanorods before and after functionalization was + 4 mV and − 14 mV, respectively.

4-MPH is a small thiolated compound; its assembly on the nanorods' surface has occurred by surface ligand exchange through the formation of a covalent bond with gold which has a well-known high affinity towards free sulfhydryl groups [45]. Thiolated ligands provide higher colloidal stability to AuNPs than other ligands that bind to the nanoparticles through hydrophobic or electrostatic attractions [45].

FTIR spectroscopy was used to confirm the surface functionalization of the nanoparticles with 4-MPH. As presented in Fig. 2, 4-MPH and 4-MPH-AuNRs demonstrated very similar FTIR spectra; both have broadband at ~ 3400 cm^{-1}, which corresponds to –OH stretching and a sharp band at ~ 1200 cm^{-1} corresponds to C–H bending in the benzene ring. Furthermore, 4-MPH showed a weak band at ~ 2560 cm^{-1} that corresponds to –SH stretching; fading of this band in the spectrum of 4-MPH-AuNRs suggests successful surface functionalization of the nanorods via S–Au covalent bond [17].

3.2 Antibacterial Activity of 4-MPH-AuNRs Against *MRSA*

3.2.1 Minimal Inhibitory and Biocidal Concentrations; MIC and MBC

Minimum inhibitory concentration (MIC) is defined as the lowest concentration of a compound or antimicrobial agent that inhibits the visible growth of a specific microorganism. Minimum bactericidal concentration (MBC) is the lowest concentration of a compound or antimicrobial agent showing no growth after exposure. MIC and MBC are commonly used in *in-vitro* studies to evaluate new compounds' antibacterial activity and to reveal bacterial resistance [46].

Our results indicate that the MIC of 4-MPH-AuNRs is estimated to be 6.25 μg/mL (Fig. 3A). Interestingly, the MBC of 4-MPH-AuNRs was the same as the MIC, indicating that the nanorods in our study have bactericidal activity towards this strain of *MRSA*. Bactericidal antibiotics actively kill the bacteria compared to bacteriostatic agents that slow or inhibit the growth of bacteria but do not kill them; generally, bactericidal agents have a ratio of MBC to MIC ≤ 4 [47]. Over the same concentration range tested for 4MPH-AuNRs, PEG-AuNRs have no antibacterial activity against the clinical strain of MRSA (Fig. 3B), moreover, 4-MPH did not demonstrate antibacterial activity against MRSA strain too.

AuNPs have shown a broad spectrum of antibacterial activity against Gram-positive and Gram-negative bacteria [48]. In addition to their chemical and physical merits, AuNRs do not develop drug resistance easily compared to

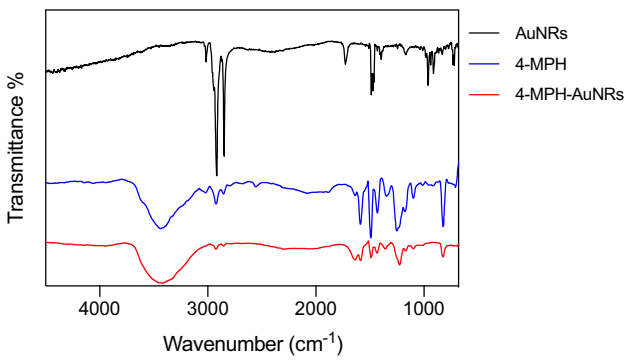

Fig. 2 FTIR spectra of AuNRs, 4-MPH, and 4-MPH-AuNRs. 4-MPH and 4-MPH-AuNRs demonstrated similar spectra. Fading of the –SH band at ~ 2560 cm^{-1} in the spectrum of 4-MPH-AuNRs suggests a successful functionalization through thiol-gold binding

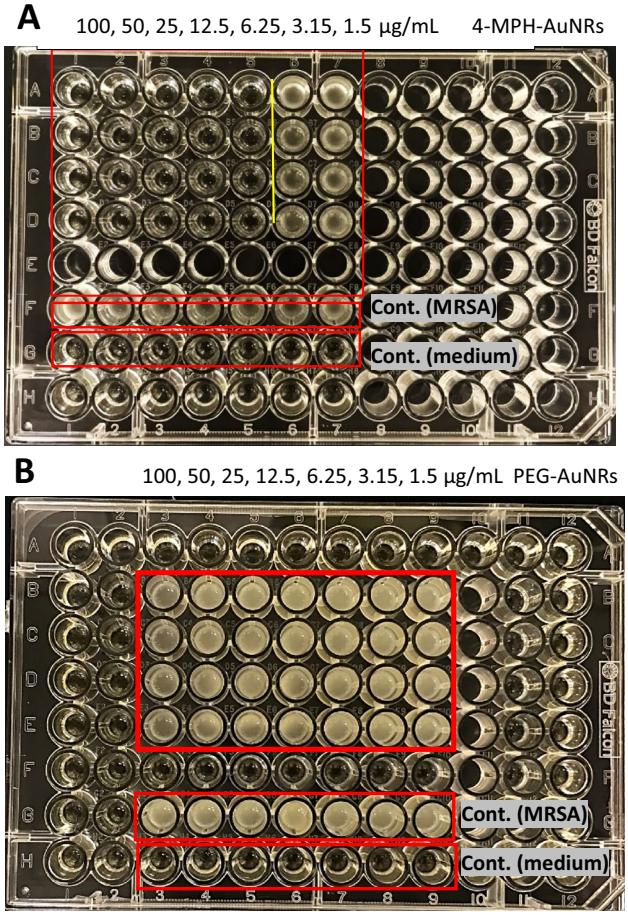

Fig. 3 MIC test in 96-well plate indicates the MIC value of 4-MPH-AuNRs (**A**) and PEG-AuNRs (**B**) at different concentrations (μg/mL) against a clinical strain of *MRSA*. The rows A-D and B-E are for the treatment of 4-MPH-AuNRs and PEG-AuNRs, respectively

conventional antibacterial agents, which is considered an interesting advantage, particularly against resistant and biofilm-producing pathogens [48, 49].

The size and shape of AuNRs have a crucial role in their biomedical responses [50, 51]; for example, nanoflowers and nanostars were shown to demonstrate considerable antibacterial activity against *S. aureus* [52]; Furthermore, nanoclusters exhibited promising antibacterial activity against different types of multidrug-resistant bacteria in a previous study [53].

On the other hand, the surface chemistry of nanoparticles has significant effects on their antibacterial activity. AuNPs conjugated to antibiotics or chemical ligands have demonstrated appreciable antibacterial activities towards a broad spectrum of Gram-positive and Gram-negative bacteria; for example, the antibacterial activity of AuNPs functionalized with Amoxicillin [54], enzyme-like activity compounds [55], chitosan [56] or supported on mesoporous silica [57] has been displayed against *S. aureus* and other bacterial strains. We previously demonstrated that AuNRs coated with a phospholipid moiety demonstrated low MIC value and high antibacterial activity compared to AuNRs coated with a cholesterol moiety against *S. aureus* strain [22].

In this study, we demonstrated for the first time the antibacterial activity of AuNRs coated with 4-MPH ligand against a clinical strain of *MRSA*, a resistant strain with a biofilm-forming ability. Generally, nanoparticles show preferential binding to Gram-positive pathogens, such as *Listeria monocytogenes*, *S. aureus,* or *Streptococcus pyrogens*, with enhanced antibacterial activity [58]. 4-MPH-AuNRs are easily synthesized and exhibit good colloidal stability.

It is worth mentioning that the adsorption of biomolecules, such as proteins and lipids on the surface of nanoparticles (formation of bio-corona) upon exposure to biological media influences the nanoparticle characteristics such as stability and reactivity. Consequently, bio-corona could affect the NPs' biological responses, cellular uptake, and toxicity [59]. Furthermore, the formation of bio-corona depends on factors such as the physicochemical properties of the nanoparticles and the physiological environment [59–61].

Although the 4-MPH-AuNRs have negative-charged surface chemistry, this does not explain their bacterial uptake or biological responses since nanoparticles acquire biocorona once exposed to the biological conditions [58, 62]. More specifically, the surface charge of 4-MPH-AuNRs was increased once exposed to the bacterial growth medium due to the formation of bio-corona around the nanoparticles, which determines their various biological responses such as cytotoxicity and cellular uptake. A recent study revealed that biomolecules could drastically affect the inhibitory effect of the nanomaterials under physiological conditions [58].

3.3 Antibiofilm Activity of 4-MPH-AuNRs Against *MRSA* Biofilm

3.3.1 Biofilm Formation

The antibiofilm activity of surface-functionalized nanorods 4-MPG-AuNRs was investigated at the MIC concentration and higher. The *MRSA* biofilm was grown on the surface of beads, and the formed biofilm was characterized by quantifying the number of bacteria/bead at different time points (Fig. 4) and SEM imaging (Fig. 5).

The bacterial CFU/bead was found to be 6.1×10^7, 7.4×10^8, and 4.12×10^9 after 24, 48, and 72 h of culturing onto the glass beads, respectively, at 37 °C (Fig. 4). The SEM images reveal the formation and attachment of the biofilm on the surface of glass beads and biofilm density formed onto the surface at each time point (Fig. 5A–D), where the highest density was obtained after 72 h of bacterial culturing (Fig. 5D).

Adherence and attachment of bacteria cells to form a biofilm on a surface is dependent on many factors, such as environmental conditions, types, and surface properties of

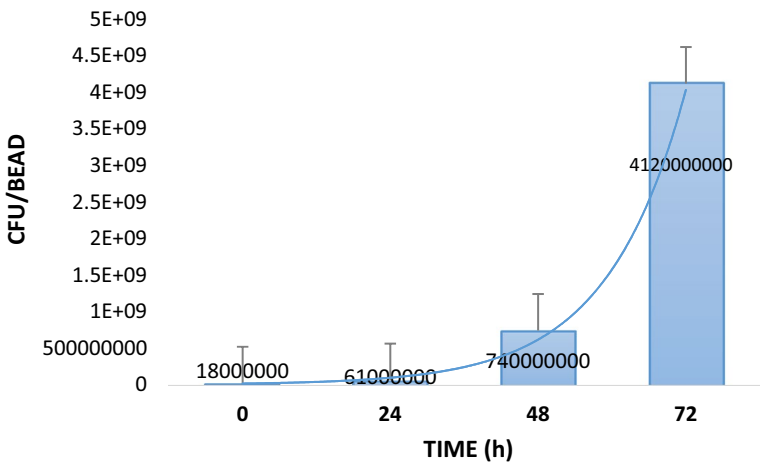

Fig. 4 Number of bacteria in the biofilm formed on glass beads at 0, 24, 48, and 72 h post-incubation

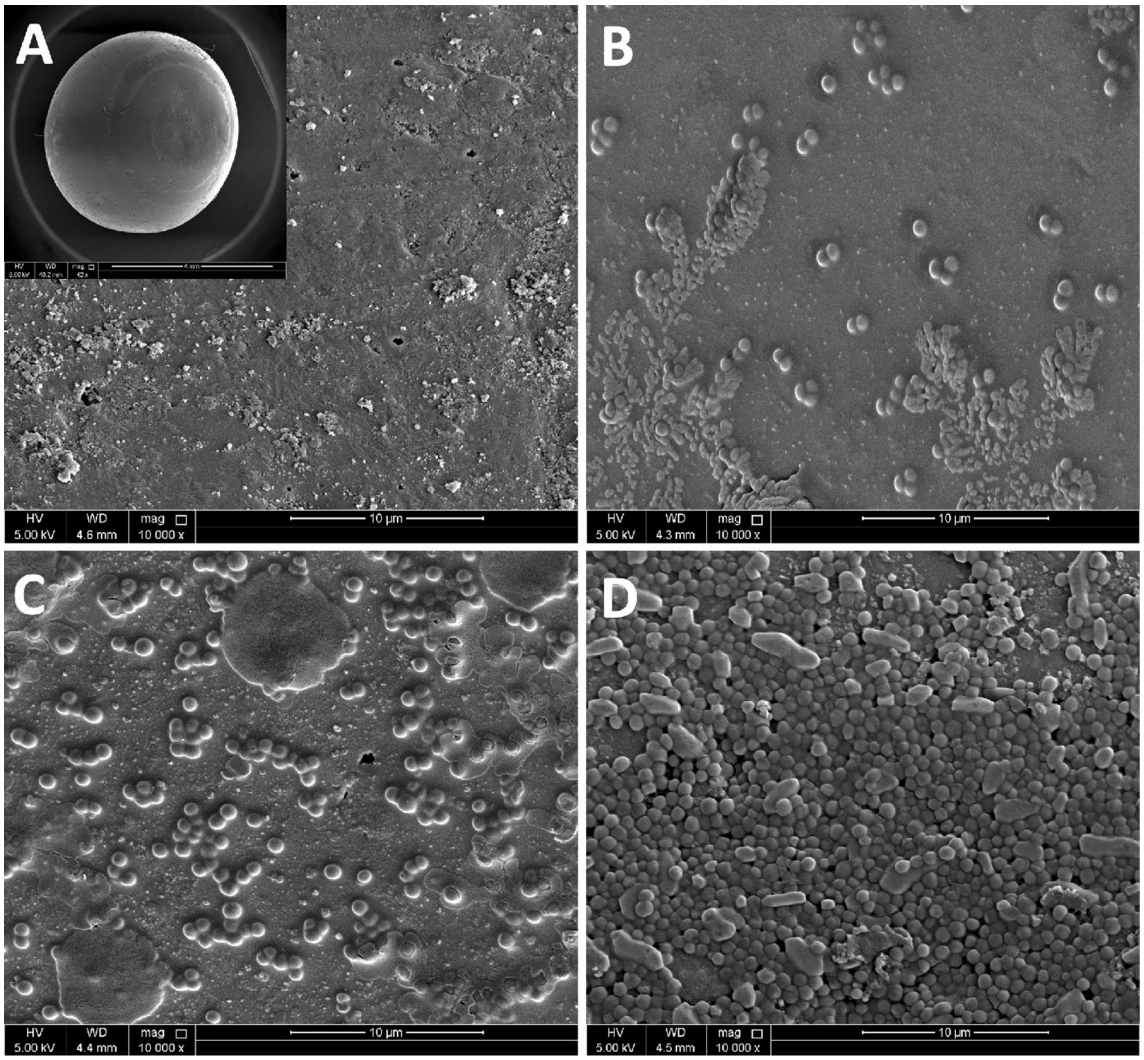

Fig. 5 SEM images of the glass bead before biofilm culturing of *MRSA* (**A**), and after 24 h (**B**), 48 h (**C**), and 72 h (**D**) of biofilm culturing onto the glass beads. The high density of bacterial biofilm was observed after 72 h

materials. Glass and other polymeric surfaces are commonly used to enhance the formation of bacterial biofilms, which produce extracellular materials that facilitate attachment and matrix formation [35].

3.3.2 Anti-biofilm Activity of 4-MPH-AuNRs Against MRSA Biofilm

The inhibition activity of the nanorods on the bacterial biofilm was estimated by calculating the percentage reduction and log-cycle reduction of the biofilm upon treatment with four different concentrations of 4-MPH-AuNRs. As described in Table 1, 4-MPH-AuNRs resulted in a ~ 1.8 − 2.90 log-cycle reduction of the viable bacterial count of the *MRSA* biofilm.

Biofilm formation of bacteria is considered one of the essential virulence factors that enhances the pathogen's colonization and infections, particularly in wound infections [63, 64]. Biofilm is a complex structure of adherent bacterial that proliferate and accumulate extracellular matrix [64]. Eradication of bacterial biofilms is considered a challenge for conventional antibiotics. Previous reports demonstrate the ability of AuNPs to inhibit or eradicate the bacterial biofilm; for example, AuNPs coated with polyethylene glycol/polyethyleneimine strongly inhibited biofilm formation of *Candida albicans* and [63]; in addition, we demonstrated previously the ability of surface-functionalized AuNRs to eradicate *Pseudomonas aeruginosa* biofilm by the photothermal mechanism of action [21]. In order to inhibit or eradicate the bacterial biofilm, nanoparticles should penetrate the bacterial biofilm and disrupt its structure; penetration into the biofilm depends on many factors such as size, shape, and surface chemistry of the nanoparticles and the biofilm characteristics and maturity [65]. The observed significant

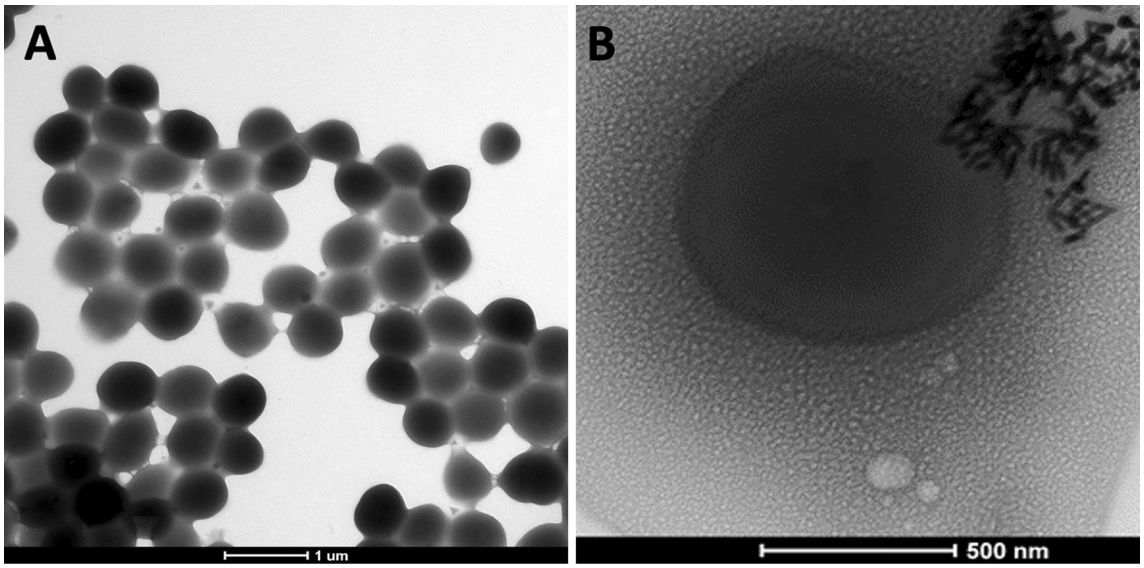

Fig. 6 SEM image of *MRSA* before (**A**) and after (**B**) treatment with 4-MPH-AuNRs for 6 h. The image shows the accumulation of the nanorods at the bacterial cell membrane with possible internalization across the bacterial cell membrane

Table 1 Percentage reduction and log-cycle reduction of viable biofilm after treatment with 4-MPH-AuNRs of different concentrations for 24 h

4-MPH-AuNRs (μ g/ml)	Conc of bacteria post-treatment (CFU/ml)	% Reduction of viable count	Log-cycle reduction
100	5×10^6	99.88	2.91
40.0	4.4×10^7	98.93	1.97
20.0	6.5×10^7	98.42	1.80
6.0	6.3×10^7	98.47	1.81

eradication of the biofilm by 4-MPH-AuNRs indicates the ability of the nanorods to penetrate efficiently into the *MRSA* biofilm and disrupt and eradicate its matrix. We hypothesize that such an effect could be related to mechanical deformation of the biofilm resulting from accumulation and adsorption of the nanoparticles at the biofilm matrix and bacterial cell membrane [66].

3.4 Cellular Uptake of AuNRs into *MRSA* by ICP-OES and SEM Imaging

In order to understand the interaction of 4-MPH-AuNRs with *MRSA* and their bacterial uptake, we quantified the percentage of bacterial uptake of the nanorods by the ICP-OES method. The results indicate that the average bacterial uptake of AuNRs inside the cell was corresponding to ~ 27% of the total amount of applied nanorods. The results demonstrate that an appreciable amount of the nanorods were internalized into bacterial cells and consequently enhanced their effect. SEM imaging of treated bacteria (Fig. 6 A–B) reveals that the nanorods were accumulated at the surface of the bacterial cells with possible internalization into the bacterial cell wall after 6 h of incubation, and eventually, cellular rupture and death. Cellular uptake of nanoparticles is essential for their biological responses and toxicity; nanoparticles have been conjugated with specific ligands to intensify their internalization into bacterial cells and, consequently, their antibacterial activity [67].

In addition to the crucial role of bio-corona in modulating the nanoparticles' cellular uptake and antibacterial mechanism of action, the nanoparticles' size plays a crucial role too. A recent study demonstrated that the antibacterial mechanism of action of nanoparticles within the size range of 80–100 nm is caused by mechanical deformation of the bacterial cell membrane due to their adsorption at the cellular membrane [66, 68]. On the other hand, the antibacterial activity of smaller nanoparticles is related to their translocation through the bacterial cell membrane and forming irreversible pores [69].

4 Conclusions

Gold nanoparticles provide promising solutions to address challenges related to bacterial resistance and decreased efficiency. 4-MPH functionalized-gold nanorods exhibited potent antibacterial and antibiofilm activities towards a clinical isolate of *MRSA*. The surface-functionalized nanorods exhibited considerable internalization into the bacterial cells, which may justify their cytotoxicity against the

bacterial biofilm. 4-MPH-AuNRs is a potential nano-system to eradicate planktonic and biofilm of *MRSA*, particularly for topical chronic wounds.

Acknowledgements The authors thank the Deanship of Scientific Research et al.-Zaytoonah University of Jordan (2020-2019/12/28) and Qatar University (BRC-2021-ID-02, QUST-2-CHS-2021-2019) for the financial funding.

Funding Open Access funding provided by the Qatar National Library. Funding was provided by Al-Zaytoonah University of Jordan (2020-2019/12/28) and Qatar University (BRC-2021-ID-02, QUST-2-CHS-2021-2019).

Declarations

Conflict of interest The authors declare no conflict of interest.

7. References

1. M. Balouiri, M. Sadiki, S.K. Ibnsouda, J. Pharm. Anal. **6**, 71 (2016)
2. N. Durán, M. Durán, M.B. de Jesus, A.B. Seabra, W.J. Fávaro, G. Nakazato, Nanomed. Nanotechnol. Biol. Med. **12**, 789 (2016)
3. R. Jayakumar, M. Prabaharan, P.T. Sudheesh Kumar, S.V. Nair, H. Tamura, Biotechnol. Adv. **29**, 322 (2011)
4. S. Bayda, M. Adeel, T. Tuccinardi, M. Cordani, F. Rizzolio, Molecules **25**, 112 (2019)
5. L. Gonzalez, R.J. Loza, K.-Y. Han, S. Sunoqrot, C. Cunningham, P. Purta, J. Drake, S. Jain, S. Hong, J.-H. Chang, J. Ocul. Pharmacol. Ther. **29**, 124 (2013)
6. P. Dallas, V.K. Sharma, R. Zboril, Adv. Coll. Interface Sci. **166**, 119 (2011)
7. H.-J. Park, S. Park, J. Roh, S. Kim, K. Choi, J. Yi, Y. Kim, J. Yoon, J. Ind. Eng. Chem. **19**, 614 (2013)
8. R. Kumar, A. Umar, G. Kumar, H.S. Nalwa, Ceram. Int. **43**, 3940 (2017)
9. M. Saeedi, M. Eslamifar, K. Khezri, S.M. Dizaj, Biomed. Pharmacother. **111**, 666 (2019)
10. N.N. Mahmoud, D.A. Sabbah, R. Abu-Dahab, D. Abuarqoub, M. Abdallah, E.A. Khalil, RSC Adv. **9**, 12718 (2019)
11. E.E. Connor, J. Mwamuka, A. Gole, C.J. Murphy, M.D. Wyatt, Small **1**, 325 (2005)
12. Pradeepa, S.M. Vidya, S. Mutalik, K. Udaya-Bhat, P. Huilgol, K. Avadhani, Life Sci. **153**, 171 (2016)
13. E. Piktel, Ł Suprewicz, J. Depciuch, S. Chmielewska, K. Skłodowski, T. Daniluk, G. Król, P. Kołat-Brodecka, P. Bijak, A. Pajor-Świerzy, K. Fiedoruk, M. Parlinska-Wojtan, R. Bucki, Sci. Rep. **11**, 12546 (2021)
14. M.M. Abdel-Kareem, A.A. Zohri, Lett. Appl. Microbiol. **67**, 465 (2018)
15. Y. Zhao, Y. Tian, Y. Cui, W. Liu, W. Ma, X. Jiang, J. Am. Chem. Soc. **132**, 12349 (2010)
16. T. Chatterjee, B.K. Chatterjee, P. Chakrabarti, Sci. Rep. **7**, 9671 (2017)
17. N.N. Mahmoud, R. Abu-Dahab, L.A. Hamadneh, D. Abuarqoub, H. Jafar, E.A. Khalil, Mol. Pharm. **16**, 4149 (2019)
18. N.N. Mahmoud, A. Albasha, S. Hikmat, L. Hamadneh, R. Zaza, Z. Shraideh, E.A. Khalil, Biomater. Sci. **8**, 1669 (2020)
19. J.R. Nicol, D. Dixon, J.A. Coulter, Nanomedicine (Lond) **10**, 1315 (2015)
20. G. Sanità, B. Carrese, A. Lamberti, Front. Mol. Biosci. **7**, 381 (2020)
21. A.G. Al-Bakri, N.N. Mahmoud, Molecules **24**, 2661 (2019)
22. N.N. Mahmoud, A.A. Alhusban, J.I. Ali, A.G. Al-Bakri, R. Hamed, E.A. Khalil, Sci. Rep. **9**, 5796 (2019)
23. N.N. Mahmoud, A.M. Alkilany, E.A. Khalil, A.G. Al-Bakri, Sci. Rep. **8**, 6881 (2018)
24. K.M. Hamad, N.N. Mahmoud, S. Al-Dabash, L.A. Al-Samad, M. Abdallah, A.G. Al-Bakri, RSC Adv. **10**, 25889 (2020)
25. V. Spampinato, M.A. Parracino, R. La Spina, F. Rossi, G. Ceccone, Front. Chem. **4**, 8 (2016)
26. K. Koç Ö, A. Üzer, R. Apak, Mikrochim Acta 187, 586 (2020).
27. P. Ruzza, A. Rosato, A. Nassi, M. Rondina, M. Zorzin, C.R. Rossi, M. Floreani, L. Quintieri, J. Med. Chem. **52**, 4973 (2009)
28. D.B. Shpakovsky, C.N. Banti, E.M. Mukhatova, Y.A. Gracheva, V.P. Osipova, N.T. Berberova, D.V. Albov, T.A. Antonenko, L.A. Aslanov, E.R. Milaeva, S.K. Hadjikakou, Dalton Trans. **43**, 6880 (2014)
29. O. Sagdic, F. Tornuk, Antimicrobial properties of organosulfur compounds, in *Dietary Phytochemicals and Microbes*. ed. by A.K. Patra (Springer, Dordrecht, 2012), p. 127
30. K.L. Mattern, C.A. Evans, J.C. Lara, Appl. Environ. Microbiol. **37**, 177 (1979)
31. P. Del Giudice, Acta Derm. Venereol. **100**, adv00110 (2020)
32. K.A. Rodvold, K.W. McConeghy, Clin. Infect. Dis. **58**(Suppl 1), S20 (2014)
33. G.F. Gad, M.A. El-Feky, M.S. El-Rehewy, M.A. Hassan, H. Abolella, R.M. El-Baky, J. Infect. Dev. Ctries. **3**, 342 (2009)
34. P.D. Stapleton, P.W. Taylor, Sci. Prog. **85**, 57 (2002)
35. J.-S. Lee, Y.-M. Bae, S.-Y. Lee, S.-Y. Lee, J. Food Sci. **80**, M2279 (2015)
36. W. Xiu, J. Shan, K. Yang, H. Xiao, L. Yuwen, L. Wang, VIEW **2**, 20200065 (2021)
37. B. Malaekeh-Nikouei, B.S. Fazly Bazzaz, E. Mirhadi, A.S. Tajani, B. Khameneh, J. Drug Deliv. Sci. Technol. **60**, 101880 (2020)
38. B.L. Scott, K.T. Carron, J. Phys. Chem. C **120**, 20905 (2016)
39. Ö.K. Koç, A. Üzer, R. Apak, Microchim. Acta **187**, 586 (2020)
40. M. Brust, M. Walker, D. Bethell, D.J. Schiffrin, R. Whyman, J. Chem. Soc. Chem. Commun. **7**, 801 (1994)
41. B.P. Khanal, E.R. Zubarev, Angew. Chem. Int. Ed. **48**, 6888 (2009)
42. N.N. Mahmoud, H. Qabooq, S. Alsotari, O.A. Tarawneh, N.H. Aboalhaija, S. Shraim, A.M. Alkilany, E.A. Khalil, R. Abu-Dahab, RSC Adv. **11**, 19956 (2021)
43. X. Ye, C. Zheng, J. Chen, Y. Gao, C.B. Murray, Nano Lett. **13**, 765 (2013)
44. X. Huang, M.A. El-Sayed, J. Adv. Res. **1**, 13 (2010)
45. M.H. Jazayeri, H. Amani, A.A. Pourfatollah, H. Pazoki-Toroudi, B. Sedighimoghaddam, Sens. Bio-Sens. Res. **9**, 17 (2016)
46. J.M. Andrews, J. Antimicrob. Chemother. **48**(Suppl 1), 5 (2001)
47. G.A. Pankey, L.D. Sabath, Clin. Infect. Dis. **38**, 864 (2004)

48. X. Gu, Z. Xu, L. Gu, H. Xu, F. Han, B. Chen, X. Pan, Environ. Chem. Lett. **19**, 167 (2021)
49. X. Zhao, Y. Jia, J. Li, R. Dong, J. Zhang, C. Ma, H. Wang, Y. Rui, X. Jiang, ACS Appl. Mater. Interfaces **10**, 29398 (2018)
50. Y.C. Dong, M. Hajfathalian, P.S.N. Maidment, J.C. Hsu, P.C. Naha, S. Si-Mohamed, M. Breuilly, J. Kim, P. Chhour, P. Douek, H.I. Litt, D.P. Cormode, Sci. Rep. **9**, 14912 (2019)
51. X. Xie, J. Liao, X. Shao, Q. Li, Y. Lin, Sci. Rep. **7**, 3827 (2017)
52. J. Penders, M. Stolzoff, D.J. Hickey, M. Andersson, T.J. Webster, Int. J. Nanomed. **12**, 2457 (2017)
53. Y. Li, J. Zhen, Q. Tian, C. Shen, L. Zhang, K. Yang, L. Shang, J. Colloid Interface Sci. **569**, 235 (2020)
54. S. Kalita, R. Kandimalla, K.K. Sharma, A.C. Kataki, M. Deka, J. Kotoky, Mater. Sci. Eng. C Mater. Biol. Appl. **61**, 720 (2016)
55. W. He, Y.T. Zhou, W.G. Wamer, X. Hu, X. Wu, Z. Zheng, M.D. Boudreau, J.J. Yin, Biomaterials **34**, 765 (2013)
56. K. Saravanakumar, A.V.A. Mariadoss, A. Sathiyaseelan, M.-H. Wang, Int. J. Biol. Macromol. **165**, 747 (2020)
57. Y. Tao, E. Ju, J. Ren, X. Qu, Adv. Mater. **27**, 1097 (2015)
58. S. Siemer, D. Westmeier, M. Barz, J. Eckrich, D. Wünsch, C. Seckert, C. Thyssen, O. Schilling, M. Hasenberg, C. Pang, D. Docter, S.K. Knauer, R.H. Stauber, S. Strieth, Biomaterials **192**, 551 (2019)
59. J. Shannahan, Nanotechnol. Rev. **6**, 345 (2017)
60. P. Chandran, J.E. Riviere, N.A. Monteiro-Riviere, Nanotoxicology **11**, 507 (2017)
61. S.J. Park, Int. J. Nanomed. **15**, 5783 (2020)
62. G. Caracciolo, O.C. Farokhzad, M. Mahmoudi, Trends Biotechnol. **35**, 257 (2017)
63. Q. Yu, J. Li, Y. Zhang, Y. Wang, L. Liu, M. Li, Sci. Rep. **6**, 26667 (2016)
64. S.C. Davis, C. Ricotti, A. Cazzaniga, E. Welsh, W.H. Eaglstein, P.M. Mertz, Wound Repair Regener. **16**, 23 (2008)
65. A.S. Joshi, P. Singh, I. Mijakovic, Int. J. Mol. Sci. **21**, 7958 (2020)
66. D.P. Linklater, V.A. Baulin, X. Le-Guével, J.B. Fleury, E. Hanssen, T.H.P. Nguyen, S. Juodkazis, G. Bryant, R.J. Crawford, P. Stoodley, E.P. Ivanova, Adv. Mater. **32**, e2005679 (2020)
67. M. Kumar, W. Tegge, N. Wangoo, R. Jain, R.K. Sharma, Biophys. Chem. **237**, 38 (2018)
68. M. Okkeh, N. Bloise, E. Restivo, L. De Vita, P. Pallavicini, L. Visai, Nanomaterials (Basel) **11**, 312 (2021)
69. E.A. Ortiz-Benítez, N. Velázquez-Guadarrama, N.V. Durán-Figueroa, H. Quezada, J.J. Olivares-Trejo, Metallomics **11**, 1265 (2019)